Vibration control of adjacent beams with pneumatic granular coupler: an experimental study

Jacek Mateusz Bajkowski[a,*], Czesław Bajer[b], Bartłomiej Dyniewicz[b], Dominik Pisarski[b]

[a]*Faculty of Production Engineering, Warsaw University of Technology, Narbutta 85, 02-524 Warsaw, Poland*
[b]*Institute of Fundamental Technological Research, Polish Academy of Sciences, Pawińskiego 5b, 02-106 Warsaw, Poland*

Abstract

A novel type of pneumatic device filled with granular material is proposed in the implementation of a switched control strategy to stabilize the vibration of slender structures. The analytically obtained control law for the airtight, elastic, granular coupler is implemented in a test structure with a relay-type control logic. In the experiment, the deformable granular coupler semi-actively damps an initially deflected pair of adjacent, aluminum beams. Two cases of initial excitation are considered, showing an improvement of up to 33 percent in vibration abatement efficiency compared to the passive case. Although this semi-active device is conceptually simple, its ease of operation and low cost should attract the attention of engineers who seek solutions that can be used to build new structures and upgrade existing ones.

Keywords: adaptive structure, pneumatic control, damping, stabilisation, granular material

1. Introduction

Typical damping techniques performed with granular materials have been studied in the literature over the years. In these techniques, a passive vibration suppression is obtained with particles placed in a container attached to the primary structure or packed in structural voids [1, 2, 3]. As the primary structure vibrates, the loose particles collide with each other and against the container walls. Non-conservative interactions such as momentum transfer, frictional deformation, internal energy dissipation, etc. facilitate the reduction in kinetic energy [4, 5].

The damping method introduced in this paper is notably different from that of typical granular dampers, which operate in a fully passive manner. The main difference between them is the restricted movement of the particles, which are no longer loosely placed in a rigid container but tightly packed in an airtight, elastic sleeve (Figure 1). The construction of a hermetic sleeve made of natural latex rubber allows controlling underpressure among tightly bounded granules. Many parameters like shape, size, material or mass ratio of the granules and sleeve may affect the efficiency, thus the issue of optimal constructional parameters is open. The dynamic control of the underpressure intensifies the jamming mechanism, allowing transition of the filling material from a fluid-like to a solid-like phase and enhancing the global rigidity of the ensemble [6]. In this paper, the authors describe the global damping properties of the granular coupler applying phenomenological approach, rather than analysing non-trivial particle interactions in the jammed state.

The proposed vibration mitigation system is composed of electromechanically controlled vacuum pump, displacement sensors and the granular dissipator. The principle of vibration abatement is based on a energy transmission controlled by sequentially coupling parallel structures of different dynamic characteristics to mistune their motion according to a state-feedback control law. The granular coupler in practice is a semi-active, deformable damper with time-dependant parameters of dissipation. The parametrical modification of the system, is often referred to as "switching times con-

*Corresponding author
Email addresses: jm.bajkowski@gmail.com (Jacek Mateusz Bajkowski), cbajer@ippt.pan.pl (Czesław Bajer), bdynie@ippt.pan.pl (Bartłomiej Dyniewicz), dpisar@ippt.pan.pl (Dominik Pisarski)

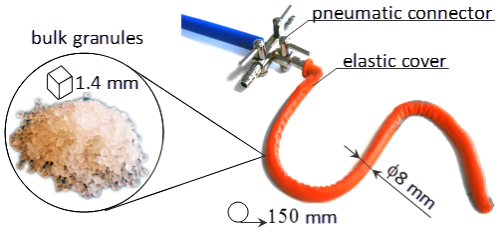

Figure 1: Experimental granular coupler (length 150 mm, ϕ8 mm) filled with cubic ABS granules ($1.4 \times 1.4 \times 1.4$ mm).

trol" [7] or "prestress-accumulation-release" strategy [8]. Usually, the switching takes place between two extreme control values, as in the "bang-bang" type of control, or between two states of the actuator, as in on-off logic.

The controlled jamming of granular materials has rather rarely been explored in vibration attenuation, since morphing of the boundary walls of the container may be difficult to achieve. Author in [9] discusses the use of a cellular structure, shape memory alloys, or electromagnets to increase the static pressure among the granules and force the jamming transition. In [10] granules were placed inside a rigid container with an adjustable position of the top lid that allowed compressing the granules and obtaining a variable stiffness. The use of a pneumatic control to increase the static pressure of a controllable granular structure covering steel beam was presented in [11]. In the following work, the concept of a new type, deformable, damping device filled with granules is presented. The obtained parametrical control policy of the pneumatically operated device is adapted for sequential coupling of slender beams, demonstrating the effectiveness of vibration abatement obtained with the prototype.

2. Investigated system

We will consider structures that can be represented by a set of linear elastic slender beams, as depicted in Figure 2. For each beam we assume a constant rectangular cross-section A, length L_1 and L_2, cross-sectional inertia I, mass density ρ and elastic modulus E. To capture the dynamics of the beams, subjected to bending, we select the Euler model. This model provides high accuracy and is relatively simple for the control purposes. The imposed assumption of linear elasticity indicates that only small and moderate loads are considered.

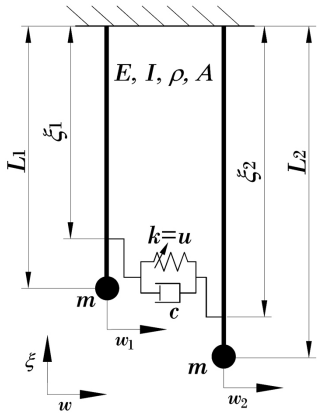

Figure 2: The investigated system of adjacent beams with Kelvin–Voigt mathematical model of the granular coupler.

The granular coupler is located at the positions ξ_1 and ξ_2 and joins the adjacent beams. As we shall demonstrate later, the selection of $\xi_1 \neq \xi_2$ is required to provide high performance for the stabilising controller. For the mathematical description, the granular coupler is represented by the Kelvin–Voigt (K–V) model, which consists of a purely viscous damper c and a purely elastic spring k. As discussed in [12], the K–V model provides a good approximation of the experimental data for a wide range of granular materials subjected to underpressure, and is easy to adapt to control and optimisation problems. A variable stiffness k is assumed for the control parameter and later denoted by u.

Let w_1 and w_2 stand for the transverse deflections of the beams (which are later measured experimentally). The system is governed by the following set of partial differential equations:

$$\begin{aligned} &\rho A\ddot{w}_1 + EIw_1'''' + \delta(\xi-\xi_1)\left[c\dot{w}_1 + k(t)w_1\right] + \\ &- \delta(\xi-\xi_2)\left[c\dot{w}_2 + k(t)w_2\right] + \delta(\xi-L_1)m\ddot{w}_1 = 0, \\ &\rho A\ddot{w}_2 + EIw_2'''' + \delta(\xi-\xi_2)\left[c\dot{w}_2 + k(t)w_2\right] + \\ &- \delta(\xi-\xi_1)\left[c\dot{w}_1 + k(t)w_1\right] + \delta(\xi-L_2)m\ddot{w}_2 = 0\,. \end{aligned} \tag{1}$$

Here, dot and prime denote differentiation with respect to time t and the space coordinate ξ, respectively. The ends of the beams that are fixed impose the following boundary conditions: $w_i(0,t) = w_i'(0,t) = w_i''(L_i,t) = w_i'''(L_i,t) = 0$, $i = 1,2$. For the initial conditions, we assume non-zero initial deflections w^0 and initial velocities $\dot{w}^0$: $w_i(\xi,0) = w_i^0(\xi)$, $\dot{w}_i(\xi,0) = \dot{w}_i^0(\xi)$, $i = 1,2$.

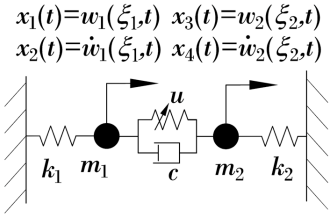

Figure 3: The reduced system of combined cantilever beams represented by coupled oscillators.

3. Control design

The stabilising controller will be based on a practical state-dependent switching law. The control strategy design and synchronisation analysis will be carried out employing the first modal approximation to (1). The reduced size of the system will enable us to perform the experimental tests with the available equipment. The proposed general methodology can be implemented in multimodal systems.

3.1. Model reduction

Let us consider the system depicted in Figure 3. Referring to Figure 2 each beam is now represented by a simple oscillator, and joined by the controlled pneumatic coupler. The parameters of the oscillators mimic the dynamics of the first natural modes of the beams. Denoting by ω the first natural frequency of the cantilever, the stiffness and the mass of the reduced system can be computed as: $k_1(\xi_1) = 3EI/\xi_1^3$, $m_1(\xi_1) = k_1(\xi_1)/\omega^2$, $k_2(\xi_2) = 3EI/\xi_2^3$, $m_2(\xi_2) = k_2(\xi_2)/\omega^2$. By introducing the state vector $x = [x_1, x_2, x_3, x_4]^T \in \mathbb{R}^4$ and the matrices

$$A = \begin{bmatrix} 0 & 1 & 0 & 0 \\ -k_1/m_1 & -c/m_1 & 0 & c/m_1 \\ 0 & 0 & 0 & 1 \\ 0 & c/m_2 & -k_2/m_2 & -c/m_2 \end{bmatrix} \qquad B = \begin{bmatrix} 0 & 0 & 0 & 0 \\ -1/m_1 & 0 & 1/m_1 & 0 \\ 0 & 0 & 0 & 0 \\ 1/m_2 & 0 & -1/m_2 & 0 \end{bmatrix} \tag{2}$$

the reduced system is governed by the following bilinear system

$$\dot{x} = A\,x + u\,B\,x\,, \tag{3}$$

with the initial condition $x(0) = [w_1^0(\xi_1), \dot{w}_1^0(\xi_1), w_2^0(\xi_2), \dot{w}_2^0(\xi_2)]^T$. The control input is assumed to be bounded by the minimum and the maximum admissible stiffness, denoted respectively by u_{min} and u_{max}):

$$u \in \mathcal{U} = [u_{min}, u_{max}] \subset \mathbb{R}_{\geq 0}\,. \tag{4}$$

3.2. Derivation of the control law

Bilinear control systems such as (3) have always had to struggle with finding efficient and robust methods for the optimal policies. No generic methods like the Linear Quadratic Regulator (LQR) can be applied here. In practice, only heuristic strategies, like Skyhook or Groundhook [13], have been successfully implemented in vehicle suspension systems or moving oscillator problems [14]. The idea behind these concepts is to stabilize the vibration by reproducing the damping forces as the system was operating with an imaginary damper that is fixed to the sky or to the ground. In practice, Skyhook or Groundhook are realized by employing vibration sensors combined with active or semi-active damping devices. Mohler in [15] presented an iterative method which is analogous to LQR. Due to the slow convergence of the procedure, the method is not eligible for real-time applications. Most of the optimal controllers for bilinear systems are implemented by using the switching times methods. In [16, 17, 18], the authors developed this method to suppress the vibration of structures subjected to traveling loads. In the present paper, a switched control strategy will be designed based on the Lyapunov's classical second method for stability. It enables to derive an explicit, robust state-feedback control law capable of real-time implementation with the use of accessible state information. Let us first introduce the energy function corresponding to the system (3): $V = \frac{1}{2} x^T Q\, x$, $Q = \mathrm{diag}(k_1, m_1, k_2, m_2)$. The time derivative of the energy function is

$$\dot{V} = x^T Q\, A\, x + u\, x^T Q\, B\, x\,. \tag{5}$$

By substituting the matrices (2) into (5) we obtain

$$\dot{V} = -c\,(x_2 - x_4)^2 - u\,(x_1 - x_3)\,(x_2 - x_4)\,. \tag{6}$$

Our goal is to design the control u^*, that provides the best instantaneous energy dissipation, i.e., $u^*(t) = \mathrm{argmin}_{u \in \mathcal{U}}\, \dot{V}(x(t))$ for all t. From (4) and (6) we conclude that

$$u^*(t) = \begin{cases} u_{max} & \text{if } (x_1(t) - x_3(t))\,(x_2(t) - x_4(t)) > 0\,, \\ u_{min} & \text{otherwise}\,. \end{cases} \tag{7}$$

By analysing the structure of $\dot{V}$, one can observe that, for a sufficiently small u_{min}, the control (7) guarantees a permanent decrease of the energy, except for the time instants when $x_2 = x_4$. Referring to LaSalle's Invariance Principle, asymptotic stability requires that the origin be the only invariant set where $x_1 = x_3$ and $x_2 = x_4$. For the considered system this condition cannot be assured, since in the case of identical oscillator parameters and identical initial conditions, the system remains conservative. The other observation concerning (6) is that a greater desynchronisation provides a better rate of the energy decrease. Thus, the key for a high performance of the designed controller lies within a proper selection of the system parameters so to avoid the state synchronisation.

A comprehensive analysis of the synchronisation of the system (3) driven by the controller (7) has been presented in [19]. In the present work, we will recall only the crucial facts allowing for a proper design of the experimental stand. Let $\epsilon = [\epsilon_1, \epsilon_2]^T$ be the relative state vector, where $\epsilon_1(t) = x_1(t) - x_3(t)$ and $\epsilon_2(t) = x_2(t) - x_4(t)$. We can define the energy function $V_\epsilon = \frac{1}{2}\epsilon^T Q_\epsilon \epsilon$, $Q_\epsilon = \mathrm{diag}(k_1 + k_2, m_1 + m_2)$, associated with the relative state dynamics:

$$\begin{aligned} \dot{\epsilon}_1 &= \epsilon_2 \,, \\ \dot{\epsilon}_2 &= -\frac{k_1}{m_1} x_1 + \frac{k_2}{m_2} x_3 - c\left(\frac{1}{m_1} + \frac{1}{m_1}\right)\epsilon_2 + \\ &- u\left(\frac{1}{m_1} + \frac{1}{m_1}\right)\epsilon_1 \,. \end{aligned} \tag{8}$$

The time derivative of the function V_ϵ can be written as follows:

$$\begin{aligned} \dot{V}_\epsilon &= -(k_1 - k_2)(x_1 + x_3)\epsilon_2 + \\ &\left[k_1\left(\frac{m_2}{m_1} - 1\right)x_1 + k_2\left(\frac{m_1}{m_2} - 1\right)x_3\right]\epsilon_2 + \\ &- c\left(\frac{1}{m_1} + \frac{1}{m_1}\right)(m_1 + m_2)\epsilon_2^2 + \\ &- u\left(\frac{1}{m_1} + \frac{1}{m_1}\right)(m_1 + m_2)\epsilon_1\epsilon_2 \,. \end{aligned} \tag{9}$$

Observe that under the control defined in (7), with sufficiently small u_{min} the sum of the terms on the two bottom lines in (9) can be either negative or zero. By taking $k_1 \neq k_2$ the first term oscillates between positive and negative values. If we assume $k_1 > k_2$ and the initial condition such that $(x_1(0) + x_3(0))(x_2(0) - x_4(0)) < 0$, then when $k_1 - k_2$ is large enough, for some time period we have $\dot{V}_\epsilon > 0$. In that period, due to the desynchronisation of the states, the system's energy V decreases very quickly. The latter change of the sign of $(x_1(0) + x_3(0))(x_2(0) - x_4(0))$ does not result in a significant loss of performance. Analogous conclusion can be drawn for the second term, when $m_1 \neq m_2$. In order to provide the best performance when applied to a real structure, the reduced stiffness values $k_1(\xi_1)$ and $k_2(\xi_2)$ should be the resultant of the expected initial condition. On the other hand, in real structures, one can rarely predict the direction of the external excitation, so a pair of controlled couplers instead of one is recommended. Let k_1', k_2' and ξ_1', ξ_2' be respectively the reduced stiffness and the fixation points of the additional coupler. The fixation points should be selected to provide that we have both $k_1(\xi_1) < k_2(\xi_2)$ and $k_1'(\xi_1') > k_2'(\xi_2')$ (or alternatively $k_1(\xi_1) > k_2(\xi_2)$ and $k_1'(\xi_1') < k_2'(\xi_2')$). In the experimental study, we will assume a single coupler. Regarding the considered initial conditions the coupler will be located at the position providing $k_1(\xi_1) > k_2(\xi_2)$.

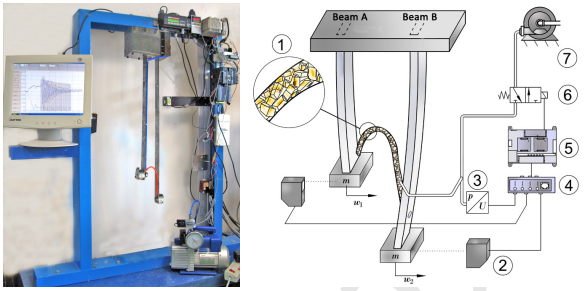

a) b)

Figure 4: Experimental test rig -a) and schematic diagram of the system -b): 1–granular coupler, 2–displacement sensors, 3– underpressure sensor, 4–data acquisition, 5–controller, 6–electrovalve, 7–vacuum pump.

4. Experimental results

The experimental configuration (Figure 4) comprises two parallel beams made of aluminum, having Young modulus 69 GPa, mass density 2.71 gcm^{-3}, shear modulus 26 GPa and Poisson's ratio 0.30. The shorter beam A is 650 mm long, and the slender beam B is 700 mm long. Both of the beams have a rectangular cross-section with a width of 25 mm and thickness 2 mm. The gap between the adjacent beams is 65 mm. One end of each beam is rigidly fixed and restrains all degrees

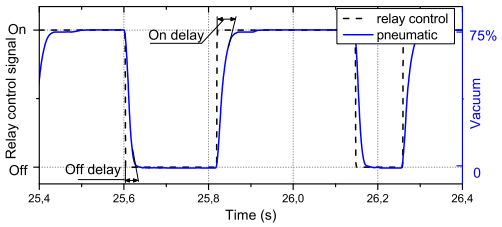

Figure 5: Electric control signal and underpressure value over time.

of freedom, while the other one is free. The tip of each beam is loaded with the mass of 370 g. A conventional natural latex rubber balloon of wall thickness in the range of 0.1 to 0.2 mm was used to form the coupler. The coupler is 150 mm long with an average outer diameter of 8 mm, and a mass of 10 g (Figure 1). The u-shaped coupler is fixed to beam A using a metal clamp at 600 mm, and to the second beam at 680 mm. The u-shape allows the coupler to be deflected when beams are approaching each other. When the beams are distancing, the coupler unbents, allowing the beams to move away from each other without the risk of being blocked by the straighten coupler. For no underpressure applied, the approximate stiffness of the coupler is 3 Nm^{-1}. For the 75 percent vacuum the stiffness was 21 Nm^{-1}. The displacement sensors were assembled to measure transverse displacements of the beams tips. The switching algorithm was adapted to a computer with digital input/output card and a programmable logic controller, responsible for switching of the electrovalve. The maximum stiffness of the coupler (u_{max}) was achieved for the activated solenoid of the normally closed valve. To minimise the time lag (delays below 0.03 s) and achieve quick pneumatic response an effective armature and underpressure accumulator were used. The shape of the electrical control signal and the underpressure value over time are presented in Figure 5.

4.1. Case I - single beam deflected

In the case I scenario, the longer beam B was initially deflected according to the shape of the first natural mode, while the beam A served the adjoint purpose. The time-history dependencies of the beams' tip horizontal displacement component are presented in Figure 6. Three operating conditions have been considered: permanently compliant, permanently stiff, and controlled coupler.

The damping factor is calculated using the half-

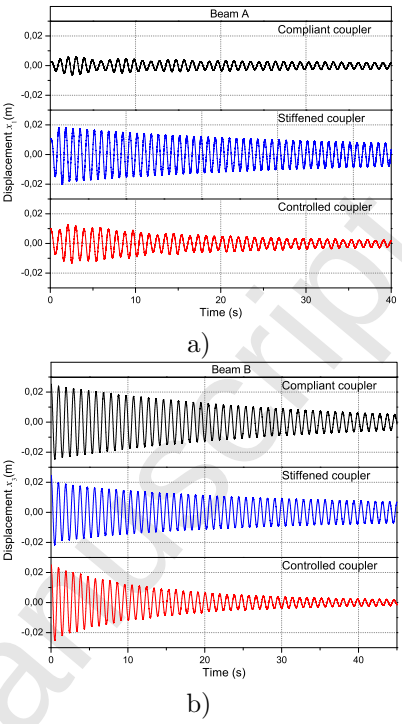

Figure 6: Vertical displacement of the tip of the beam A -a), and the beam B -b) for the case I.

power bandwidth method and denoted ζ_A and ζ_B for the respective beams (Figure 7 a and b). The unitless amplitude represents relative strength of the harmonic component of the source signal.

When the coupler is permanently compliant small damping is present. The initially excited beam B suffers from large amplitudes of displacement, as only a part of the energy is transferred to beam A. When the coupler is permanently stiff, the relative displacement between the beams becomes nearly zero. The rigidly connected beams behave like a combined system, performing a synchronized vibration with large amplitudes of displacement and low damping factor ($\zeta_A = \zeta_B = 0.018$).

When the controlled coupling is performed, vibrations of the excited beam B are being damped in the shortest time. During the first stage of motion, the beams are out of synchronisation, and thus the energy dissipation is very effective. Synchronisation takes place close to the origin, which is adverse for the efficiency of the vibration abatement. The damping factors $\zeta_A = 0.018$ and $\zeta_B = 0.020$ are increased by 50 percent for beam A and 43 percent for beam B when compared to the passive case.

To provide some general quantitative comparison,

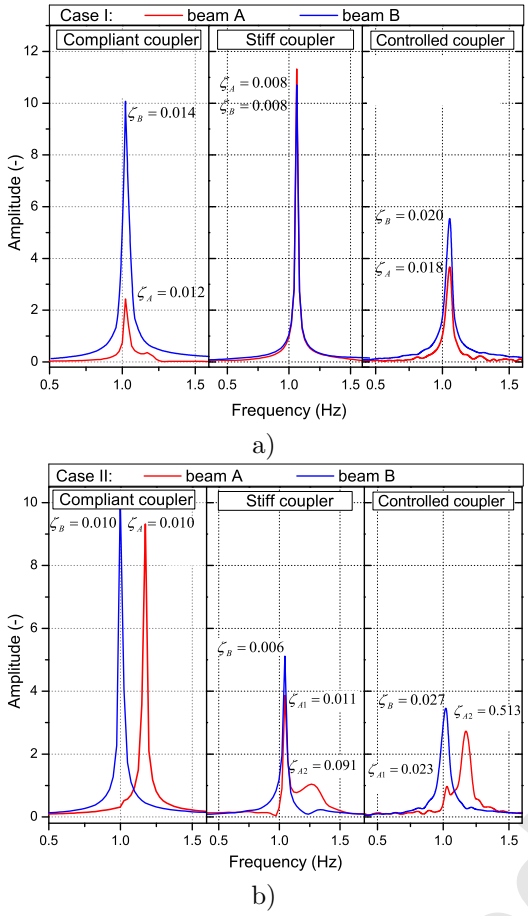

Figure 7: Frequency response and damping factor of the beams for case I -a), and case II -b).

the value of the energy metric corresponding to the potential energy of the beams is calculated:

$$\hat{J} = \sum_{n=1}^{N} J(n) = \frac{1}{2} \sum_{n=1}^{N} \left(x_1^2(n) + x_2^2(n) \right), \qquad (10)$$

where n is the sample number, and N is the total number of samples across the 40 s interval. The energy metric normalized to the value obtained for the compliant coupler is listed in Table 1 for case I and II. The controlled coupling outperforms the compliant case by 33 percent.

4.2. Case II - both beams deflected

In the second case tip of each beam was displaced by 15 mm in opposite directions and shaped according to the first modal form. For the compliant coupler, the vibration of each beam is slightly damped over time. Since the state-space trajectories overlap (Figure 8), the lowest damping factor values are noted ($\zeta_A = \zeta_B = 0.010$).

Table 1: Normalized energy metric.

	Compliant	Stiffened	Controlled
Case I $\hat{J}$	1.00	1.50	0.67
Case II $\hat{J}$	1.00	0.30	0.27

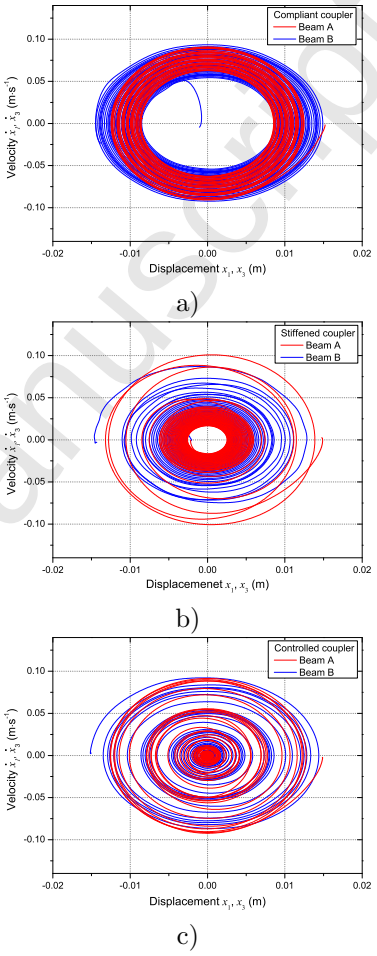

Figure 8: State-space trajectories of the considered system for compliant -a), stiffened -b) and controlled coupler -c) for case II.

When the beams are joined by the permanently stiff coupler and deflected in opposite directions, a part of the energy is dissipated in the process of deformation, as the beams are compressing the coupler when approaching each other. The system is unsynchronized (see the orbits), so the performance of the stiff coupler is now more effective than for the case I. One can observe a minor presence of the higher vibration modes for beam A (Figure 7b) with damping factor $\zeta_{A2} = 0.091$. Once again, the con-

trolled system is the most effective one, as greatest desynchronisation is observed. After several cycles the trajectories of the controlled system converge to the equilibrium. Note that the amplitude of the first peak for beam A is now lower than amplitude for the second mode, as the second mode dominates the vibration abatement. The damping factors are increased up to $\zeta_{A1} = 0.023$, $\zeta_{A2} = 0.513$ and $\zeta_B = 0.027$. In terms of the assumed energy metric the controlled case outperforms the stiffened case by 10 percent (Table 1).

5. Conclusions

Free vibrations of two adjacent beams connected by a special granular damping interface were considered. The obtained analytical model is capable of capturing the features of this new type of simple damping device. The experimental results confirm the analytical computations and demonstrate that switching stiffness of the robust granular coupler can be very effective in mitigating vibrations. The best rate of the decrease of energy is provided when the movement of the adjacent structures is kept unsynchronized. Each of the controlled variants in the experimental cases I and II outperformed the passive solutions. A properly scaled device of this type can support the existing damping solutions if specific constructional factors and fail-safe design are taken into account. Depending on the scale of the device and dedicated application, generation of the underpressure may be achieved utilizing or modifying pumps and generators already installed in civil structures or vehicles, allowing for an effective energy consumption.

6. Acknowledgements

The research leading to these results has received funding from the Polish National Science Center under grant agreement 2013/11/D/ST8/03437 and 2015/17/B/ST8/03244.

References

[1] M. Sanchez, G. Rosenthal, L. Pugnaloni, Universal response of optimal granular damping devices, J Sound Vib 331 (2012) 4389–4394. doi:10.1016/j.jsv.2012.05.001.

[2] Z. Lu, X. Lu, S. F. Masri, Studies of the performance of particle dampers under dynamic loads, J Sound Vib 329 (2010) 5415–5433. doi:10.1016/j.jsv.2010.06.027.

[3] T. Szmidt, R. Zalewski, Inertially excited beam vibrations damped by vacuum packed particles, Smart Materials and Structures 23 (10) (2014) 105026. doi:10.1088/0964-1726/23/10/105026.

[4] H. V. Panossian, Structural damping enhancement via non-obstructive particle damping technique, J Vib Acoust 114 (1992) 101105. doi:10.1115/1.2930221.

[5] G. H. Ristow, Critical exponents for granular phase transitions, Europhys Lett 40 (6) (1997) 626–630. doi:10.1209/epl/i1997-00514-3.

[6] M. E. Cates, J. P. Wittmer, J. P. Bouchaud, P. Claudin, Jamming, force chains and fragile matter, Phys Rev Lett 81 (1998) 1841–1844. doi:http://dx.doi.org/10.1103/PhysRevLett.81.1841.

[7] J. Onoda, T. Endo, H. Tamaoki, N. Watanabe, Vibration suppression by variable-stiffness members, AIAA Journal 29 (6) (1991) 977–983. doi:10.2514/3.59943.

[8] A. Mroz, A. Orlowska, J. Holnicki-Szulc, Semi-active damping of vibrations: Prestress accumulation-release strategy development, Shock Vib 17 (2010) 123–136. doi:http://dx.doi.org/10.3233/SAV-2010-0502.

[9] J. A. Rongong, G. R. Tomlinson, Amplitude dependent behaviour in the application of particle dampers to vibrating structures, in: 46th AIAA/ASME Structures, Structural Dynamics and Materials Conference, Austin, Texas, 2005, pp. 1–9. doi:10.2514/6.2005-2327.

[10] C. X. Wong, J. A. Rongong, Control of particle damper nonlinearity, AIAA Journal 47 (4) (2009) 953–960. doi:10.2514/1.38795.

[11] J. M. Bajkowski, R. Zalewski, Transient response analysis of a steel beam with vacuum packed particles, MECH RES COMMUN 60 (2014) 1–6. doi:10.1016/j.mechrescom.2014.04.004.

[12] J. M. Bajkowski, B. Dyniewicz, C. I. Bajer, Damping properties of a beam with vacuum-packed granular damper, J Sound Vib 341C (2015) 74–85. doi:10.1016/j.jsv.2014.12.036.

[13] D. Karnopp, M. Crosby, R. Harwood, Vibration control using semi-active force generators, ASME Journal of Engineering for Industry 96 (1974) 619–626. doi:10.1115/1.3438373.

[14] D. Giraldo, S. J. Dyke, Control of an elastic continuum when traversed by a moving oscillator, J STRUCT CONTROL HLTH 14 (2002) 197–217. doi:10.1002/stc.152.

[15] R. R. Mohler, Bilinear Control Processes, Academic Press, New York, 1973.

[16] D. Pisarski, C. Bajer, Smart suspension system for linear guideways, J INTELL ROBOT SYST 62 (3-4) (2011) 451–466. doi:10.1007/s10846-010-9450-7.

[17] D. Pisarski, Distributed control design for structures subjected to traveling loads, MATH PROBL ENG 2015 (2015) 1–12. doi:http://dx.doi.org/10.1155/2015/206870.

[18] B. Dyniewicz, R. Konowrocki, C. Bajer, Intelligent adaptive control of the vehicle-span/track system, MECH SYST SIGNAL PR 58-59 (2015) 1–14. doi:10.1016/j.ymssp.2014.12.007.

[19] D. Pisarski, C. I. Bajer, B. Dyniewicz, J. M. Bajkowski, Vibration control in smart coupled beams subjected to pulse excitations, J Sound Vib 380 (2016) 37–50. doi:10.1016/j.jsv.2016.05.050.